Supporting Information

Morita et al. 10.1073/pnas.1005938107

SI Materials and Methods

Cell Cultures. HeLa, 293T, GHD-1, and HOS cells were maintained in DMEM supplemented with 10% FCS. For immunofluorescence experiments, HeLa or GHD-1 cells were seeded onto coverslips and transfected with siRNA at 30–50% confluence.

Expression Vectors. Expression vectors used in these studies are summarized in Table S2.

siRNA Design and Testing. The sequences of all siRNA constructs used in this study are provided in Table S1. siRNA target sequences (19nt+d(TT) overhangs) were designed using the Dharmacon siDESIGN Center (Thermo Fisher Scientific Inc.). siRNAs used against VPS4A and VPS4B were designed, validated, and reported previously (1). Between 4 and 10 siRNAs that targeted each ESCRT-III protein were tested for efficacy and specificity (Fig. S1 and Table S1). Antibodies against both human VPS4 proteins and all human ESCRT-III proteins were obtained or developed (Table S3) and used in Western blots to determine the efficacy of target protein depletion. However, antibodies against CHMP4C did not detect the endogenous protein, apparently owing to low affinity and/or low protein levels, and the efficacy of CHMP4C silencing was therefore tested using exogenously expressed, epitope-tagged protein. Where appropriate, siRNA specificities were tested by examining the levels of related ESCRT-III family members (Fig. S1). The following criteria were used to select siRNAs for further study: (*i*) efficient silencing of the target protein, (*ii*) target protein specificity (in cases where human ESCRT-III families have multiple family members), and (*iii*) maximal cell division phenotypes. Red asterisks in Figs. S1 and S3 and Table S1 denote siRNAs that were used to obtain the data reported in the paper. Note that (*i*) In two cases, siRNAs against a targeted protein also depleted another family member to some degree (CHMP4B siRNA 617 and VPS4B siRNA 1191), and (*ii*) in every case, the reported phenotypes were reproduced using a second, different siRNA against each target protein (black asterisks in Figs. S1 and S3 and Table S1). Data from both siRNAs against CHMP2A are reported in Fig. S3 to demonstrate that the unusual phenotype observed upon CHMP2A depletion was observed for multiple different siRNAs. Note, however, that the second siRNA against CHMP2A yielded a higher percentage of cells with multiple centrosomes (similar to the phenotype seen for VPS4B depletion), in addition to the monopolar phenotype observed for the first siRNA. This observation suggests that these two phenotypes may be closely linked. The effects of depleting VPS4B were tested in four different human cell types (HeLa, GHD-1, 293T, and HOS). Similar phenotypes were observed in every cell type, but the phenotypes were more penetrant in HeLa (Figs. 1–3) and GHD-1 (Fig. S5 *A*–*C*), than in 293T and HOS cells (Fig. S5*A*).

siRNA Transfections. HeLa, GHD-1, 293T, or HOS cells in 6-well plates (2-mL culture volume) or 12-well plates (containing glass coverslips for microscopy experiments)(1-mL culture volume) were transfected twice with 20-nM siRNA duplexes at 24-h intervals using Lipofectamine RNAi MAX. Cells were harvested and analyzed after an additional 24 h except where specifically noted.

Antibody Production. Antibody sources and working dilutions are summarized in Tables S3 and S4. Antibodies against pure recombinant CHMP1B, CHMP2A, and CHMP3 proteins expressed in *E. coli* were raised in New Zealand White Rabbits (Covance, Inc.). Details of ESCRT-III protein expression, purification, and characterization have been described (2).

Immunofluorescence of Fixed Cells. siRNA-treated HeLa or GHD-1 cells were fixed with 3% paraformaldehyde (10 min, 25 °C) or 100% methanol (10 min, −20 °C for samples stained with anti-γ-Tubulin or anti-Aurora A antibodies). Fixed cells were incubated for greater than 2 h with primary antibodies diluted in PBS containing 0.1% Triton X-100 (PBST) and 3% BSA. Antibody dilutions and associated fixation methods are given in Table S4. Cells were washed 3 times with PBST, incubated with secondary antibodies (diluted in PBST with 3% BSA, 2 h, 25 °C) and/or with SYTOX Green (1 μM; Invitrogen) and then washed 3 times with PBST. Alexafluor488, 594, 647, or SYTOX Green signals were detected using a FV300 IX81 confocal microscope (Olympus) with 488-, 543-, and 633-nm excitation wavelengths. Note that VPS4A (Fig. 5), VPS4B (Fig. S6), and IST1 (3) all exhibited similar localization patterns. Analogous studies were not performed for other ESCRT-III proteins because our antibodies were not of sufficient quality to localize the endogenous proteins reliably and because terminal tags/fusion constructs typically inactivate ESCRT-III proteins (4, 5).

Flow Cytometry Analyses of Cellular DNA Content. Following siRNA treatment, HeLa, 293T, HOS, or GHD-1 cells were treated with trypsin, collected, and resuspended in 0.3 mL PI solution (50 μg PI/mL in PBS, 0.1% Triton X100, 0.25 mg RNase/mL, 30 min). Ten thousand PI-positive cells were counted with a FACScan fluorescence-activated cell sorter (FACScan; BD Bioscience), and peak volumes were analyzed using Modifit LT v2.0 software. Results shown in Fig. 1B represent the average of two experiments, and the error bars show ranges. Results shown in Fig. S5*A* represent the mean of three experiments ± SD.

Cell Death Assay. Following siRNA treatment, HeLa cell morphology was analyzed by light microscopy. Cells with highly convoluted/blebbed plasma membranes were judged to be undergoing cell death, whereas tightly adhered, flat cells or smooth, rounded cells were judged to be normal. Results shown in Fig. S5*D* represent the average of two experiments, and the error bars show ranges.

Time-Lapse Imaging of Living Cells. HeLa cells stably expressing YFP-α-Tubulin and H2B-mCherry were created by transduction with MLV-based retroviral vectors [pQCXIN; BD Bioscience (Clontech)] that expressed the two fluorescent fusion proteins. Vector stocks were created by cotransfecting the packagable pQC-YFP-α-Tubulin or pQC-H2B-mCherry expression vectors (6 μg) with expression vectors for Gag-Pol (PGag-Pol, 4 μg) and the VSV-G envelope [pMD.G envelope, 2 μg (6)] into 293T producer cells (3×10^6 cells/10-cm dish) using polyethylenimine (PEI). 36 h post-transfection, vector-containing supernatants were harvested and filtered (0.45 μm) (Millipore).

HeLa cells (2×10^6 cells/10 cm dish) were then incubated for 12 h with 5 mL of vector-containing culture media supplemented with polybrene (8 μg/mL). Following sequential transductions with the YFP-α-Tubulin and H2B-mCherry vectors, YFP- and mCherry-positive cells were sorted by FACSVantage SE High Speed Cell Sorter (BD Bioscience); >95% of purified cells expressed both YFP-α-Tubulin and H2B-mCherry. These cells were then replated [2×10^4 cells/well in a four-well Lab-Tek II chambered coverglass (Nalge Nunc International)], and incubated at 37 °C with 5% CO_2. Cells were transfected twice with siRNAs against ALIX, VPS4B, CHMP2A, or with a control siRNA (20 nM, Lipofectamine RNAi Max; Invitrogen). Immediately following the second siRNA transfection, cells were imaged within an Oko lab microscope chamber

(37 °C, 5% CO_2) using an Olympus IX81 microscope (Orca ER CCD; Hamamatsu and Motorized XY stage; Prior Scientific), UPLANSAPO 40× NA 0.90 objective, using YFP (2427A) and mCherry (TRITC-A) filters (Semrock). Images were acquired every three minutes using the MetaMorph v7.02 software (Molecular Devices Corp.).

Quantification of Defects in Mitosis and Cytokinesis. Data shown in Figs. 2 *B* and *C* and 3 *B*, *D*, and *E* and Figs. S3*B* and S5 *B–C* are the averages from three experiments, ± SD. ≥100 cells were analyzed in each experiment, except for the data in Fig. 2 *B* and *C* and Fig. S3*B*, where fewer cells were counted.

Cells with multiple and fragmented nuclei. Cells were stained with SYTOX Green to visualize the DNA/nuclei and were scored as having fragmented nuclei if they had multiple small or interconnected nuclei (Fig. 2*A*, example #3) or as multinucleated if they had multiple nuclei of normal size (see example #1).

Midbodies. Cells were stained with anti-α-Tubulin to facilitate the identification of cells that were connected by midbodies (Fig. 2*A*, example #2).

Unaligned chromosomes. Cells were judged to be in mitosis with unaligned chromosomes if (*i*) chromosomes were condensed but not aligned along at the metaphase plate (SYTOX Green staining), (*ii*) phase contrast images showed that the cells were "rounded up" (e.g., see the cell in Fig. 4 panel 1, column 3 at the 33–87 min time points), and (*iii*) cells were not apoptotic as judged by nuclear and cellular morphology.

Centrosome number. Cells were stained with anti-Pericentrin (a centrosomal marker) and the numbers of centrosomes per cell were counted. Note that in ALIX- and CHMP3-depleted cells, centrosomes were only counted in cells that had single nuclei. This procedure was used because the majority of the cells in these cultures were multinuclear (4C-16C DNA content), and therefore had multiple centrosomes because they failed to complete abscission (rather than owing to aberrant centrosomal amplification events). During interphase, control cells typically had two distinct centrosomes (red puncta in Fig. 3*A Top Left*), with only small percentages of cells exhibiting single or multiple centrosomes per cell (see quantification in Fig. 3*B*).

Centrosome volume. Centrosomes in anti-Pericentrin stained HeLa cells were reconstructed in 3D from thin Z-stacked confocal images (0.2-μm slices). Centrosome reconstructions and volumes were calculated using the Volocity 3D Imaging software (Improvision, Inc.). At least 40 centrosomes were reconstructed for each condition, and measured volumes were binned in multiples of 0.25 μm^3 (Fig. 3C).

Quantification of time-lapse movies. Measurements for Fig. 4 *C–E* were made from time-lapse movies of living HeLa cells that expressed YFP-α-Tubulin and H2B-mCherry. Measurements were averaged from three different experiments (± SD), and the total number of measurements made in each case is given within the graphs of Fig. 4. To compile the data shown in Fig. 4*C*, the duration of mitosis was measured as the time interval between initiation of chromosome condensation and chromosome segregation. In Fig. 4*D*, mitosis was judged to have failed if visual inspection clearly revealed improper chromosome alignment and segregation, including asymmetric segregation into daughter cells. Finally, in Fig. 4*E*, abscission was judged to have failed if the cleavage furrow or midbody dissolved and the nascent daughter cells coalesced back into a single cell with multiple or fragmented nuclei. Note that cells lacking ALIX, VPS4B, or CHMP2A also underwent apoptosis somewhat more frequently than control cells (Fig. S5*D*).

Time-Course of Centrosome Amplification. HeLa cells were seeded onto coverslips in a 12-well dish and transfected with siRNA against VPS4B or an irrelevant control as described above. Samples were fixed in methanol every 6 h beginning with the first transfection (t = 0 h), continuing through the second transfection (t = 24 h), and concluding 66 h from the first transfection. Cells were stained with anti-Pericentrin and anti-γ-Tubulin antibodies, and the number of centrosomes was counted by microscopy. Mitotic and interphase cells were counted separately, and only those structures that stained with both antibodies were counted as centrosomes. Three counts of 100 cells each were averaged ± SD.

1. Kieffer C, et al. (2008) Two distinct modes of ESCRT-III recognition are required for VPS4 functions in lysosomal protein targeting and HIV-1 budding. *Dev Cell* 15:62–73.
2. Bajorek M, et al. (2009) Structural basis for ESCRT-III protein autoinhibition. *Nat Struct Mol Biol* 16:754–762.
3. Bajorek M, et al. (2009) Biochemical analyses of human IST1 and its function in cytokinesis. *Mol Biol Cell* 20:1360–1373.
4. Howard TL, Stauffer DR, Degnin CR, Hollenberg SM (2001) CHMP1 functions as a member of a newly defined family of vesicle trafficking proteins. *J Cell Sci* 114:2395–2404.
5. von Schwedler UK, et al. (2003) The protein network of HIV budding. *Cell* 114:701–713.
6. Onishi M, et al. (1996) Applications of retrovirus-mediated expression cloning. *Exp Hematol* 24:324–329.

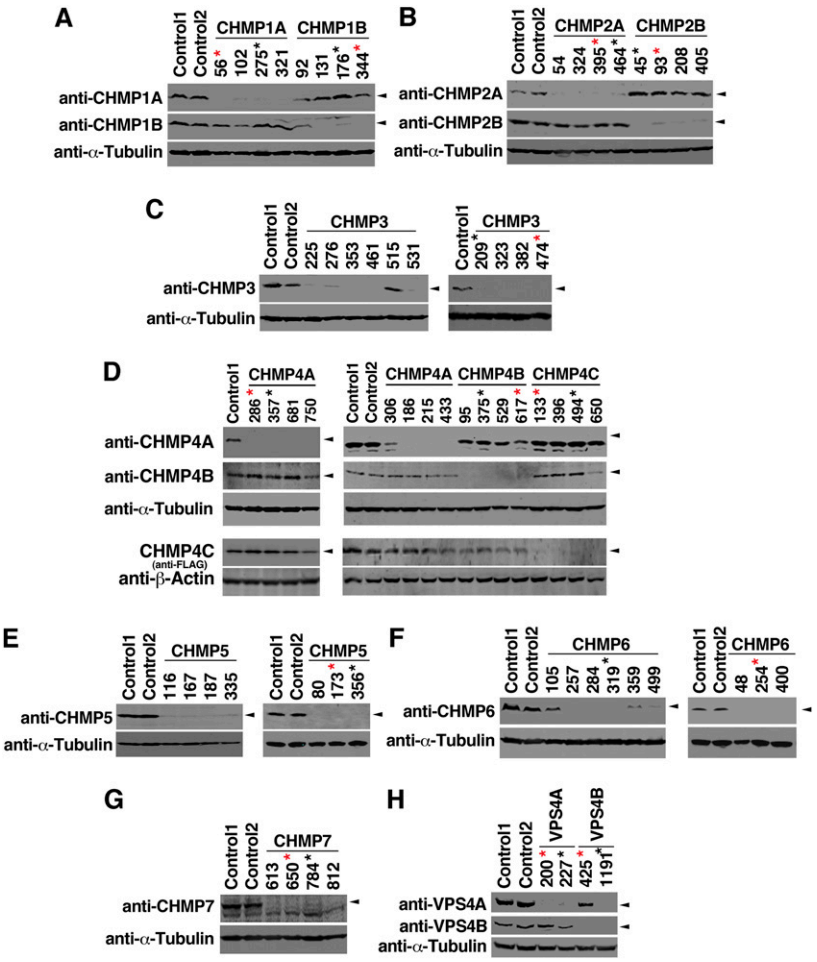

Fig. S1. siRNA depletion of ESCRT-III and VPS4 proteins. (*A–H*) Western blots showing protein levels in cells treated with siRNA to deplete endogenously expressed ESCRT-III and VPS4 proteins (*A–C*, *E–H*, and *D Upper* two panels); anti-ESCRT-III or -VPS4 antibodies) or exogenously expressed CHMP4C-FOS (*D Bottom* panel, anti-FLAG). Antibodies are identified to the left of each blot, and α-Tubulin and/or α-Actin were used as loading controls. The first one or two lanes in each blot show protein levels in cells treated with irrelevant siRNAs. Subsequent lanes show cells treated with siRNAs designed to deplete the designated proteins. Numbers denote the first nucleotide of the siRNA target site within the coding region of the target mRNA, and siRNA sequences are provided in Table S1. (*A*) CHMP1A/B, (*B*) CHMP2A/B, (*D*) CHMP4A/B/C, and (*H*) VPS4A/B demonstrate that siRNAs against one ESCRT-III/VPS4 family member generally did not deplete related family members, although the $CHMP4B_{617}$ siRNA partially depleted CHMP4A, and $VPS4B_{1191}$ depleted VPS4A. siRNAs were also tested for toxicity by coexpressing another gene product (HIV-Gag) and assaying its expression level. Asterisks indicate siRNAs that were chosen for further study: red asterisks designate siRNAs used in all figures within the main paper, and black asterisks designate siRNAs used to confirm each phenotype (e.g., Fig. S3). Relevant ESCRT-III proteins are denoted by closed arrows.

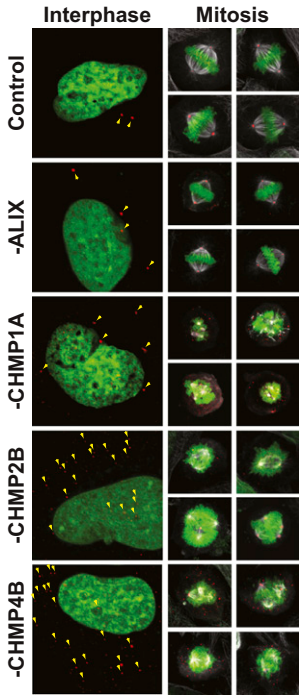

Fig. S2. Centrosomal defects induced by depletion of representative ESCRT-III proteins. Z-stacked confocal images of HeLa cells stained for DNA (SYTOX Green) and centrosomes (red, anti-Pericentrin) in interphase cells (*Left*) or mitotic cells (additionally stained for α-Tubulin (white), *Right*), following treatment with a control siRNA (panel 1), or depletion of ALIX (control, panel 2) or ESCRT-III proteins (panels 3–5).

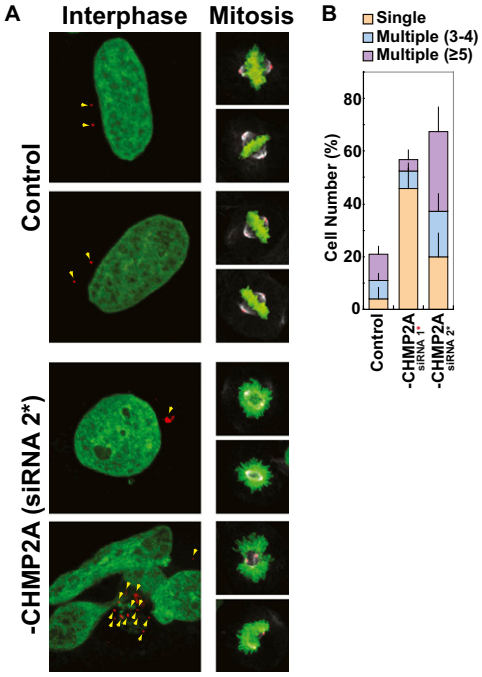

Fig. S3. Confirmation of centrosomal defects induced by depletion of CHMP2A. (*A*) Confocal images of HeLa cells stained for DNA (SYTOX Green) and centrosomes (red, anti-Pericentrin) in interphase cells (*Left*), and additionally stained for α-Tubulin (white) in mitotic cells (*Right*), following treatment with a control siRNA (panels 1–2), or with an alternative siRNA (Fig. S1 and Table S1, black asterisk) to deplete CHMP2A (panels 3–4). (*B*) Centrosome numbers in control or CHMP2A-depleted HeLa cells.

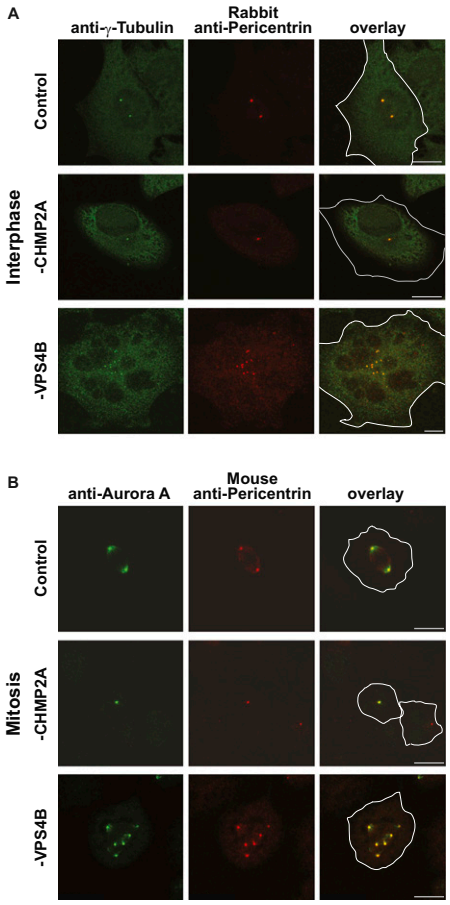

Fig. S4. Confirmation of centrosomal staining. (*A*) Confocal images of interphase HeLa cells stained for two centrosomal markers (mouse anti-γ-Tubulin, green, *Left*; and rabbit anti-Pericentrin, red, *Center*; with the two images overlayed, *Right*). Costaining with both markers was observed for nearly all centrosomes in control (row 1) or CHMP2A- (row 2) or VPS4B-depleted cells (row 3). (*B*) Confocal images of mitotic HeLa cells stained for two additional centrosomal markers (rabbit anti-Aurora A, green, *Left*; and mouse anti-Pericentrin, red, *Middle*; with the two images overlayed, *Right*), for control, CHMP2A-, or VPS4B-depleted cells as in *A*. Note that antibodies against Pericentrin in *A* and *B* were from different species and reacted with different epitopes, supporting the specificity of the centrosomal staining. (Scale bar =20 μm.)

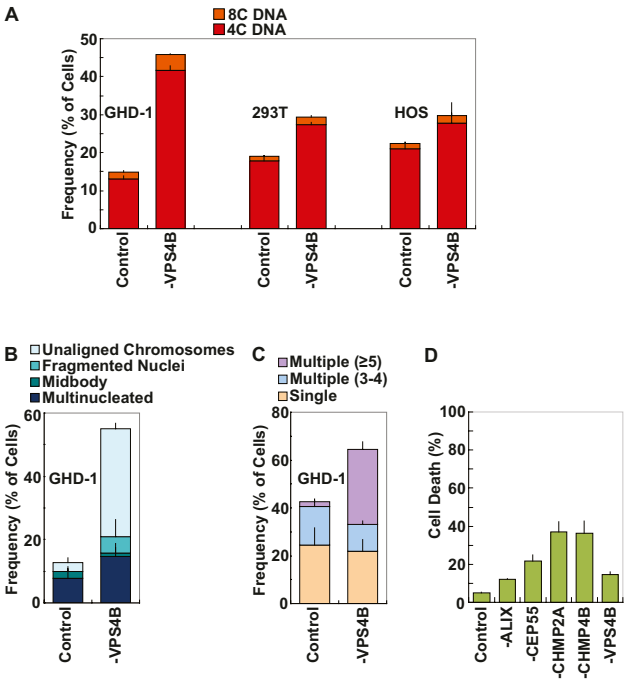

Fig. S5. Mitotic and centrosomal defects in GHD-1, 293T, and HOS cells upon depletion of ESCRT-III/VPS4 proteins, and cell death associated with ESCRT-III/VPS4 depletion. Cellular DNA content (*A*), cell morphology (*B*), and centrosome number (*C*) abnormalities upon depletion of VPS4B were examined in GHD-1 (*A*–*C*), 293T (*A* only), or HOS cells (*A* only). Experiments and data analyses were analogous to the experiments shown for HeLa cells in Figs. 1*B*, 2 *B*–*C*, and 3*B*, respectively, with the exception of (*A*), where values are the mean of three experiments ± SD. (*D*) HeLa cells depleted of the indicated proteins were observed microscopically and scored for the percentage of dead/dying cells ($n = 2 \pm$ range); ≥100 cells were counted in each experiment.

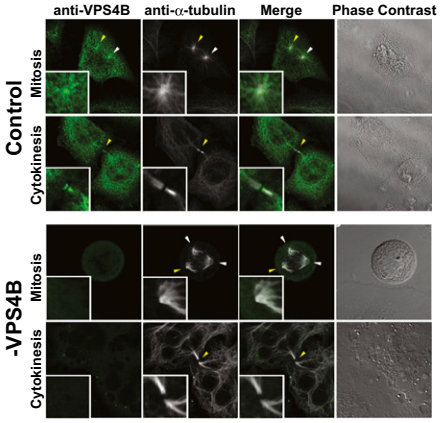

Fig. S6. Localization and specificity of antibody detection of endogenous VPS4B during different stages of the cell cycle. Fluorescent microscopic images showed that VPS4B and VPS4A (Fig. 5) proteins exhibit similar localization patterns. Representative images show localization of endogenous VPS4B (anti-VPS4B, green, columns 1 and 3) and microtubules (anti-α-Tubulin, white, columns 2 and 3) during mitosis (row 1) or cytokinesis (row 2) in cells treated with a control siRNA. Note that VPS4B concentrates at the centrosome during mitosis and at the midbody during cytokinesis. Images in rows 3 and 4 show cells depleted of VPS4B, demonstrating the specificity of antibody staining and the accumulation of multiple spindles (row 3). Centrosomes and midbodies are highlighted with arrows, and magnified insets correspond to regions highlighted by yellow arrows.

Table S1. siRNA sequences used in this study

Protein		First nucleotide	Sense sequence	RefSeq
CHMP1A	*	56	CCAAGAAGGCGGAGAAGGAtt	NM_002768.2
		102	GAAGGCCCUUCUGCAGAAAtt	Isoform 2
	*	275	UGACCAAAGCCCUGGACAAtt	
		321	GGUCUCCUCAGUGAUGGACtt	
CHMP1B		92	CCGAAAAGGCCAAAAUUAAtt	NM_020412.4
		131	ACAUGGAAGUUGCGAGGAUtt	
	*	176	AGAACCAGGCGGUGAAUUUtt	
	*	344	UGGACAAAUUCGAGCACCAtt	
CHMP2A		54	CCAGAGGGCCCUGAACCGUtt	NM_014453.2
		324	GGCCAUGGGCACCAUGAACtt	
	*	395	AGGCAGAGAUCAUGGAUAUtt	
	*	464	AAGAUGAAGAGGAGAGUGAtt	
CHMP2B	*	45	GGAACAGAAUCGAGAGUUAtt	NM_014043.3
	*	93	UCGAGCAGCUUUAGAGAAAtt	
		208	AAACAGAAGACGAGAACUUtt	
		405	GGAAAUGACUGAAGAAAUGtt	
CHMP3		225	CAAGCUGUAUGCAUCCAAAtt	NM_016079.2
		276	GAACCAGCUCGCGGUCUUGtt	Isoform 1
		353	UGAAGAUUCCAGAGAUUCAtt	
		461	AGGAAGAAAUGGAGGAAGAtt	
		515	UUACAGCAGGGGCCUUGGGtt	
		531	GGGCAAAGCACCCAGUAAAtt	
	*	209	CAAGGAAGGCUGUGAGCAAtt	
		323	CAGAAGUGAUGAAGGCCAUtt	
		382	AGGGAGUUGUCCAAAGAAAtt	
	*	474	GGAAGAAGCAGAAAUGGAAtt	
CHMP4A	*	286	AAGUAUGGGACCAAGAAUAtt	NM_014169.2
	*	357	GGCACAAACUGACGGGACAtt	
		681	AGAAGAACCCUCAGUCAAAtt	
		750	GGAUGAAGAUGAAGAAGCAtt	
		306	GAGAGCUGCCCUACAGGCUtt	
		186	UGAAGAAGCAAUACAGAAAtt	
		215	CAGAGAAGAUACUGAUCAAtt	
		433	GUCCUUCGUACCAUGGAGCtt	
CHMP4B		95	CGGAAGAGAUGUUAAGCAAtt	NM_176812.4
	*	375	CGAUAAAGUUGAUGAGUUAtt	
		529	GACAAGAAUUUGCUGGAAAtt	
	*	617	AGAAAGAAGAGGAGGACGAtt	
CHMP4C	*	133	AAUCGAAUCCAGAGAGAAAtt	NM_152284.3
		396	GCAAGAGAUCACAGAGCAAtt	
	*	494	UGGCAGAACUUGAAGAAUUtt	
		650	GGGCAGAAGAAGAGGAUGAtt	
CHMP5		116	AUGCUGAGCUAGUGAAGUAtt	NM_016410.4
		167	CUGCAAAGAAUAUGGUCAAtt	
		187	CAGAAAGCCUUGCGAGUUUtt	
		335	GAGUAAAGGAAAUGAAGAAtt	
		80	GAGCAGAAUCCAUUGACAAtt	
	*	173	AGAAUAUGGUCAAGCAGAAtt	
	*	356	CAUACAAGCAAGUGAAGAUtt	
CHMP6		105	GAGGAUCGCCCAGCAGCUGtt	NM_024591.4
		257	CCAUGGUUCAGAGUAUUGAtt	
		284	AGAUCGAAAUGAAAGUGAUtt	
	*	319	GGAAAUGAGUGUCUGAACAtt	
		359	UUGAAGAGGUGGAGAGGAUtt	
		499	CAAAUAGAGCUGCCAGAGGtt	
		48	GGACAAGGCCAUCCUGCAAtt	
	*	254	AGGCCAUGGUUCAGAGUAUtt	
		400	GUGGAGUACCAGCGGCAAAtt	
CHMP7		613	CAGAAGGAGAAGAGGGUCAtt	NM_152272.3
	*	650	GGGAGAAGAUUGUGAAGUUtt	
	*	784	GCAGAGAGGUGUAAAGAAGtt	
		812	GGGCAUGCCGAGCAGGAAAtt	
VPS4A	*	200	CCGAGAAGCUGAAGGAUUAtt	NM_013245.2

Table S1. Cont.

Protein		First nucleotide	Sense sequence	RefSeq
	*	227	GCAAAGAGAAACACGGCAAtt	
VPS4B	*	425	CCAAAGAAGCACUGAAAGAtt	NM_004869.3
	*	1,191	GGAUGUCCCUGGAGAUAAAtt	
CEP55	*	43	GGAUCGAAGCCUAGUAACUtt	NM_018131.4 Isoform1
ALIX	*	417	CCUGGAUAAUGAUGAAGGAtt	NM_013374.4 Isoform1
LucGL2 (control1)			CGUACGCGGAAUACUUCGAtt	
QIANC (control2)			UUCUCCGAACGUGUCACGUtt	

Table S2. Plasmid constructs

Plasmid name	Internal ID	Backbone	Cloning sites	Epitope tags	Source
pQC.YFP.α-Tubulin	WISP08-204	pQCxIN	BamHI, MfeI/EcoRI	N,YFP	Clontech
pQC.H2B.mCherry	WISP08-205	pQCxIN	BamHI, MfeI/EcoRI	C,mCherry	HeLa genomic DNA
pGag-Pol	WISP07-127				1
pMD.G	WISP03-279				1
pCAG.MCS2.FOS	WISP08-103	pCAG.MCS			gift from Robert A. Lamb (Northwestern University, Evanston, IL)
pCAG.CHMP4C.FOS	WISP08-88	pCAG.MCS2	KpnI, XhoI	C,FLAG-One-STrEP	2

1. Onishi M, et al. (1996) Applications of retrovirus-mediated expression cloning. *Exp Hematol* 24:324–329.
2. von Schwedler UK, et al. (2003) The protein network of HIV budding. *Cell* 114:701–713.

Table S3. Antibodies used for Western blotting

Antigen	Source	Membrane	Blocking	Dilution	Source
CHMP1A	Rabbit	Nitrocellulose	0.5% milk	1/500	gift from Stanley M. Hollenberg (Oregon Health Sciences University, Portland, OR)
CHMP1B	Rabbit	PVDF	5.0% milk	1/250	UT592
CHMP2A	Rabbit	Nitrocellulose	0.5% milk	1/250	UT589
CHMP2B	Rabbit	PVDF	5.0% milk	1/1,000	Abcam (ab33174)
CHMP3	Rabbit	Nitrocellulose	0.5% milk	1/250	UT552
CHMP4A	Rabbit	PVDF	5.0% milk	2 μg/mL	Santa Cruz (H-52)
CHMP4B	Rabbit	Nitrocellulose	0.5% milk	1 μg/mL	Santa Cruz (C-12)
CHMP5	Rabbit	Nitrocellulose	0.5% milk	1/1000	gift from Diane McVey Ward (University of Utah, Salt Lake City, UT)
CHMP6	Rabbit	PVDF	5.0% milk	1/500	UT464
CHMP7	Goat	PVDF	5.0% milk	2 μg/mL	Santa Cruz (C-19)
VPS4A	Rabbit	PVDF	5.0% milk	1/500	UT289
VPS4B	Rabbit	PVDF	5.0% milk	1/500	UT292
FLAG	Mouse	PVDF	5.0% milk	0.2 μg/mL	Sigma-Aldrich (M2)
α-Tubulin	Mouse	PVDF	5.0% milk	1/5,000	Sigma-Aldrich (DM1A)
β-Actin	Rabbit	PVDF	5.0% milk	1/1,000	Bethyl Labratories (A300-491A)

Table S4. Antibodies used for immunofluorescence

Antigen	Source	Fixation	Dilution	Source
VPS4A	Rabbit	Paraformaldehyde	1/25	UT289
VPS4B	Rabbit	Paraformaldehyde	1/25	UT292
Pericentrin	Rabbit	PFA or methanol	1/500	Novus Biological (NB100-68277)
Pericentrin	Mouse	Methanol	1/500	Abcam (ab28144)
Aurora A	Rabbit	Methanol	1/500	Abcam (ab12875)
γ-Tubulin	Mouse	Methanol	1/500	Sigma-Aldrich (GTU88)
α-Tubulin	Mouse	Paraformaldehyde	1/1000	Sigma-Aldrich (DM1A)

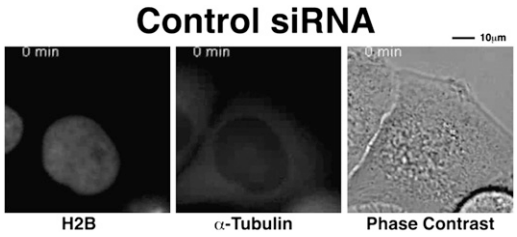

Movie S1. Time-lapse video showing cell division in a single cell treated with a control siRNA. Experiments shown in this and all subsequent movies were performed on stably transfected HeLa cells that expressed fluorescent chromatin (H2B-mCherry, *Left* in each synchronized set) and fluorescent microtubules (YFP-α-Tubulin, *Center*). Phase contrast images are provided (*Right*). Arrows highlight cells that are undergoing mitosis, and letter designations are coded to highlight the following events or defects: (a) normal mitosis, (b) arrested midbodies, (c) multiple spindles, (d) formation of fragmented nuclei, (e) aberrant monopoles, and (f) empty daughter cells lacking DNA. Elapsed times are given within each video.

Movie S1

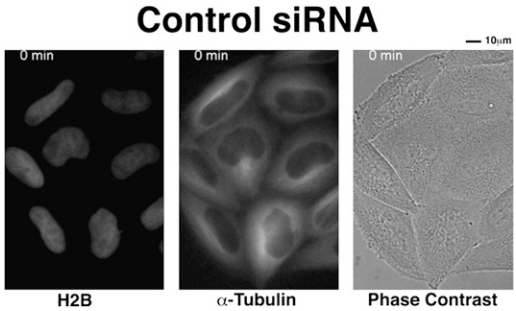

Movie S2. Time-lapse video showing cell division in a field of cells treated with a control siRNA.

Movie S2

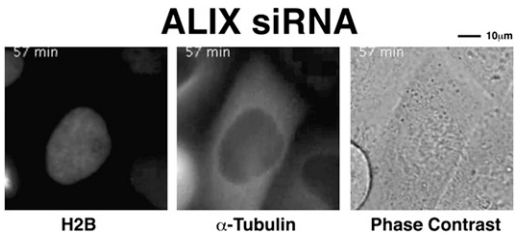

Movie S3. Time-lapse video showing cell division in a cell depleted of ALIX.

Movie S3

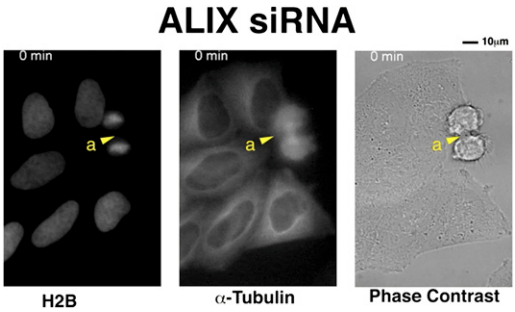

Movie S4. Time-lapse video showing cell division in a field of cells depleted of ALIX.

Movie S4

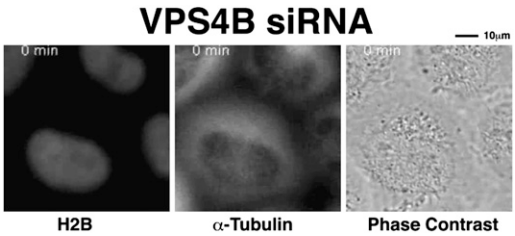

Movie S5. Time-lapse video showing cell division in a cell depleted of VPS4B.

Movie S5

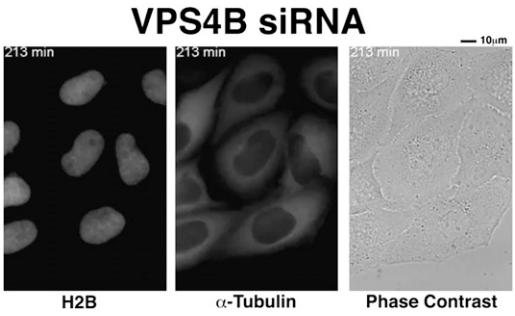

Movie S6. Time-lapse video showing cell division in a field of cells depleted of VPS4B.

Movie S6

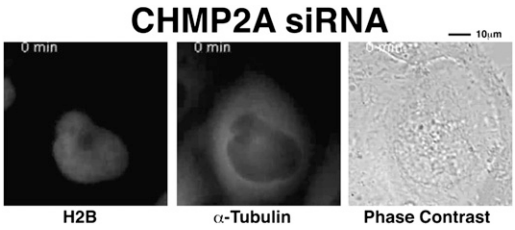

Movie S7. Time-lapse video showing cell division in a cell depleted of CHMP2A.

Movie S7

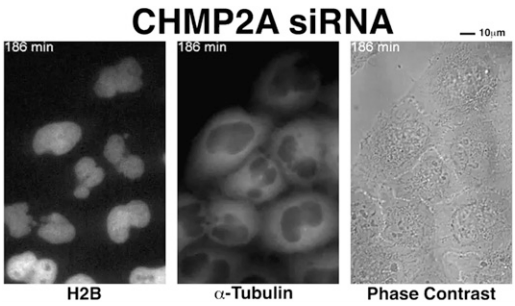

Movie S8. Time-lapse video showing cell division in a field of cells depleted of CHMP2A.

Movie S8